C505/9/011

Development of a CAE-Tool for the Design of Flight Control and Hydraulic Systems

by D Scholz, *Technical University Hamburg-Harburg, Germany*

SYNOPSIS

Generic, ready-to-use preliminary design methodologies for aircraft utility systems, made available by means of a Computer Aided Engineering tool do not exist. An attempt is made to apply principles used in preliminary aircraft design to preliminary design of utility systems. This is demonstrated for the flight control and hydraulic system. An overview is given on calculations of control surface hinge moments and deflection rates, optimization of flight control configurations and hydraulic system steady state calculations. Detailed information is given on the preliminary design methodology for hydraulic linear flight control actuation systems.

NOTATION

This is a list of key variables for preliminary actuator design, other variables are explained at first occurrence in the text.

A	piston area	[m^2]
c_a	aerodynamic load coefficient, $c_a = F/x$	[N/m]
c_h	hydraulic stiffness of cylinder	[N/m]
c_q	flow gain	[m^2/s]
c_{qp}	$c_{qp} = c_q / c_p$	[$m^5/(Ns)$]
c_p	pressure gain	[N/m^3]
c_{rl}	attachment stiffness: ram to load	[N/m]
c_{rs}	attachment stiffness: ram to structure	[N/m]
d	damping coefficient	[Ns/m]
D	damping ratio	[-]
e	error	[m]
F	load	[N]
h	effective moment arm	[m]
k	controller gain	[A/m], [-]
k_I	gain of first stage of electro-hydraulic servo-valve	[m/A], [-]

k_l flow coefficient for laminar flow orifice, $k_l = q / \Delta p$ [$m^5/(Ns)$]
k_t flow coefficient for turbulent flow orifice, $k_t = q / \Delta p^{0.5}$ [$m^3/(s \cdot Pa^{0.5})$]
K bulk modulus [N/m^2]
m moving mass [kg]
M_c closed loop amplitude ratio [-]
M_e error amplitude ratio [-]
M_m gain margin [-]
M_o open loop amplitude ratio [-]
N describing function [-]
p_l load pressure, $p_l = F/A$ [N/m^2]
p_r return pressure [N/m^2]
p_s supply pressure [N/m^2]
p_0 working pressure, $p_0 = p_s - p_r$ [N/m^2]
q flow [m^3/s]
T time constant of first stage of electro-hydraulic servo-valve [s]
V_0 total volume of one actuator chamber (piston in mid position) [m^3]
x piston position [m]
x_c commanded piston position [m]
x_{max} piston stroke [m]
y valve spool position [m]
y_{max} valve spool stroke [m]
Φ_c closed loop phase [deg]
Φ_m phase margin [deg]
Φ_o open loop phase [deg]
ω input angular frequency [1/s]
ω_n characteristic angular frequency [1/s]
ω_M gain margin frequency [1/s]
ω_Φ phase margin frequency [1/s]
$\hat{}$ amplitude of respected value
for k_2, ε, μ, U, V, W see Chapter 3 .

1 INTRODUCTION

Flight control and hydraulic systems are just two examples of utility systems (also known as fundamental, basic or general systems) of an aircraft. Utility systems provide fuel, power and essential comfort to crew and passengers and contain a large amount of what could be termed avionics. Nevertheless, pure avionic systems are not considered to be utility systems (1). Utility systems are defined and grouped by the *Air Transport Association of America* in ATA Specification 100 (2). Following this ATA-breakdown, each system is identified by its ATA-chapter number. **Table 1** lists utility systems by their ATA-chapter number.

Utility systems in modern civil transport aircraft have reached high technical and economic importance. Without them the aircraft would not even leave the ground. Utility systems

together with avionic systems account for about one third of total aircraft production costs. Much knowledge and experience was gathered by manufacturers and suppliers during past decades in the preliminary design of aircraft systems. Nevertheless, it seems that for many utility systems, generic and generally accepted preliminary design methodologies do not exist - not to speak of Computer Aided Engineering (CAE) tools for these design activities.

This is very much in contrast to preliminary aircraft design. Text books and computer programs by *Roskam* (3), (4) and *Raymer* (5), (6) are just two examples of an approach in preliminary aircraft design where generic methodologies are offered as printed medium and ready-to-use CAE tools.

Here, an attempt is made to apply principles used in preliminary aircraft design to preliminary design of utility systems. A generic design methodology for aircraft utility systems should as much as possible directly calculate required system parameters. Only when a direct solution seems not to be feasible, simulation techniques should be applied. Two utility systems - the flight control and hydraulic system - are used to demonstrate this approach. Following an overview of required calculation steps, detailed information is given in this paper on the preliminary design methodology for flight control actuation systems. Present work at the Technical University Hamburg-Harburg is geared towards the development of a CAE tool offering ready-to-use design methodologies for flight control and hydraulic systems. The CAE tool is already applied for hydraulic system analysis of a research aircraft under construction with *Daimler-Benz Aerospace Airbus GmbH*. Furthermore, the CAE tool will be applied in the predevelopment of the next generation Airbus aircraft.

Table 1: Utility Systems by ATA-Definition (2).

ATA-Chapter	Description	ATA-Chapter	Description
21	air conditioning	30	ice and rain protection
24	electrical power	32	landing gear
25	equipment furnishings	33	lights
26	fire protection	35	oxygen
27	flight control	36	pneumatic
28	fuel	38	water / waste
29	hydraulic power	49	airborne auxiliary power

2 GENERAL PROCEDURE FOR THE LAYOUT OF FLIGHT CONTROL AND HYDRAULIC SYSTEMS

Preliminary design of aircraft utility systems is based on data obtained from preliminary aircraft design as given in the Aircraft Definition Note. The CAE tool presently under development at the Technical University Hamburg-Harburg will, for now, include calculations

for activities as shown in **Fig. 1**. Supported are the preliminary design of flight control actuation systems and the layout of the aircraft hydraulic systems. The design of actuation systems requires the notion of the maximum hinge moment, control surface deflection rates with required hinge moments at these defection rates and the available size of the installation space for flight control actuators. The actuators have to be designed into the available installation space. The design of the aircraft hydraulic systems is based on an optimised flight control configuration. A proposed hydraulic system can be checked and optimised by a steady state calculation of network parameters as a function of various load combinations. As in aircraft design, solutions are evaluated by means of their cost effectiveness. For this purpose, a method to calculate the Direct Operating Costs (DOC) for aircraft utility systems was developed. For further information on aircraft system DOCs see (7).

2.1 Control surface hinge moments

Control surface hinge moments *HM* for elevator, aileron and rudder are calculated from hinge moment derivatives c_h , air density ρ , true air speed v , control surface area S_f and control surface chord c_f at aerodynamic mean chord of the main surface to which the control surface is mounted.

$$HM = \frac{1}{2}\rho v^2 \cdot C_h \cdot S_f \cdot c_f \tag{1}$$

$$C_h = C_{h_0} + C_{h_\alpha} \cdot \alpha + C_{h_\delta} \cdot \delta \tag{2}$$

α is the angle of attack of the surface. δ is the control surface deflection angle. c_{h0} is the hinge moment derivative for $\alpha = \delta = 0$. $c_{h,0}$ is often unknown in preliminary design. In this case $c_{h,0}$ has to be set to zero. $c_{h,\alpha}$ and $c_{h,\delta}$ are the partial derivatives of the hinge moment with respect to α respectively δ. In preliminary design, measured hinge moments are generally not available. When maximum hinge moments are available for an aircraft similar to the one under investigation, these hinge moments should be scaled to the new size. If the engineer is faced with a new design, hinge moment derivatives can be estimated from *DATCOM* (8) or *ESDU* (9).

The maximum elevator hinge moment is calculated for large civil transport category aircraft from requirements given in FAR 25.255 or JAR 25.255 (10). FAR/JAR 25.255 require in this context sufficient hinge moment capabilities of the elevator to achieve specified manoeuvres. These manoeuvres at true air speeds v and resulting horizontal tail angles of attack α and elevator deflection angles δ yield hinge moments *HM* from equations (1) and (2). α and δ are calculated based on FAR/JAR 25.255 as outlined in **Fig. 2**. This calculation yields a maximum elevator hinge moment *HM* for elevator up and for elevator down. The maximum hinge moment for actuator sizing depends on the effective moment arm between actuator and control surface in the respective up or down position. Calculations of maximum elevator hinge moments *HM* showed that *HM* is strongly influenced by horizontal tailplane runaway speed.

Maximum aileron hinge moments are calculated from manoeuvres given in FAR/JAR 25.349. These manoeuvres are specified originally in FAR/JAR for structural loads but serve as well for hinge moment calculation. Hinge moments *HM* are determined from equations (1) and (2) with manoeuvres flown at a true air speeds v , wing angles of attack α and aileron deflection angles δ . α and δ are calculated based on FAR/JAR 25.349 as outlined in **Fig. 3.** In the same way as for elevator hinge moments, this calculation yields a maximum aileron hinge moment *HM* for aileron up and for aileron down. The maximum hinge moment for actuator sizing depends again on the effective moment arm in the respective up or down position.

Maximum rudder hinge moments generally occur for multi engined aircraft as a result of an engine failure just after take-off. The asymmetric thrust due to the failing engine must be compensated by maximum rudder deflection $\delta_{r,max}$ and a side slip angle β. The side slip angle is restricted by a maximum bank angle of 5° (FAR/JAR 25.149). A proper preliminary sizing of the vertical tail and the rudder has to make sure that there is no need to exceed the maximum bank angle. The side slip angle follows from a summation of moments about the yaw axis:

$$\beta = \frac{1}{C_{N_\beta}} \cdot \left(\frac{N_T \left(\frac{N_D}{N_T} + 1 \right)}{\frac{\rho}{2} \cdot v_{MC}^2 \cdot S \cdot b} - C_{N_{\delta_r}} \cdot \delta_{r_{max}} \right) \tag{3}$$

with $N_T = N_{T,crit} = T_{outboard} \cdot y_{outboard}$. (T: trust of failing critical (outboard) engine; y: distance from centre line to the critical engine. N_D / N_T : drag-to-thrust-ratio of the engine. $N_D / N_T = 0.25$ for a windmilling engine with high bypass ratio. For data on further engine types see (11). $C_{N,\beta}$ the yawing-moment-due-to-sideslip derivative and $C_{N,\delta,r}$ the yawing-moment-due-to-rudder-deflection derivative can be calculated from (11). S : wing area, b : wing span, v_{MC} : minimum control speed. If v_{MC} is not know set $v_{MC} = 1.2 \cdot v_s$ (FAR/JAR 25.149) where v_s is the stall speed. This calculation yields a maximum aileron hinge moment *HM* for the rudder when inserting β for α and $\delta_{r,max}$ for δ in equation (2).

In contrast to hinge moment derivatives for elevator, aileron and rudder, handbook methods do seem not to be available for spoiler hinge moment calculation. A review of spoiler related data from literature and aircraft manufacturers (12) led to two equations for spoiler hinge moment estimation. The maximum spoiler hinge moment $HM_{sp,ext}$ for an extended spoiler can be estimated from an aircraft dive speed v_D and related maximum permissible surface extension δ_{sp} :

$$HM_{sp_{ext}} = C_D \cdot \frac{\rho}{2} \cdot v_l^2 \cdot S_{sp} \cdot \frac{c_{sp}}{2} \cdot \sin^2 \delta_{sp} \quad . \tag{4}$$

Conservation of momentum yields a drag coefficient $C_D = 2.0$. More realistic values for C_D are between $C_D = 1.5$ for spoilers with small spanwise extension to $C_D = 1.8$ for spoilers with large spanwise extension or for neighbouring spoilers being simultaneously extended. ρ : air

density, S_{sp} : spoiler surface area, c_{sp} : spoiler chordwise extension. v_l is the airspeed at the spoiler position. v_l is higher than the true airspeed of the aircraft v. If v_l is unknown, $v_l = 1.14 \cdot v$ can be used as a good first estimate.

A hinge moment is also necessary to keep the retracted spoiler in place. This hinge moment is caused by a difference of pressures above (p_u) and below (p_l) the spoiler. The pressure below the spoiler is approximately the average of the pressures present on the upper and lower surface of the wing ($p_u + p_l$) / 2 . The maximum spoiler hinge moment $HM_{sp,ret}$ is therefore calculated from ($p_u - p_l$) / 2 and can be estimated from an assumed elliptical lift distribution and a factor K_{sp} to account for the chordwise lift distribution. K_{sp} was determined by fitting spoiler hinge moment data from the aircraft manufacturer to the derived equation

$$HM_{sp,ret} = K_{sp} \cdot \frac{c_{sp} \cdot S_{sp} \cdot W \cdot n_z}{c(y_{sp}) \cdot b \cdot \pi} \cdot \sqrt{1 - \left(\frac{2 \cdot y_{sp}}{b}\right)^2} \quad . \tag{5}$$

$K_{sp} = 1.5$ produced a good match. Variables in equation (5) are: c_{sp} : spoiler chord, S_{sp} : surface area of spoiler, W : aircraft weight, n_z : load factor, y_{sp} : spanwise location of spoiler, $c(y_{sp})$: wing chord at spanwise location of spoiler, b : wing span.

2.2 Control surface deflection rates

Following a rule of thumb (13), a first estimate of a control surface deflection rate $\dot{\delta}$ is

$$\dot{\delta} = \frac{\delta_{max}}{\Delta t} \qquad with \quad \Delta t = 1\ s\ .$$

δ_{max} is the deflection angle to move the control surface from the neutral position to full hard over. More precisely, required control surface deflection rates should be calculated from flying qualities as defined in military specification MIL-F-8785C (14) or military standard MIL-STD-1797 (15).

Aileron deflection rates can be calculated from requirements of MIL-F-8785C Chapter 3.3.4 or MIL-STD-1797 Chapter 4.5.8. The military standard specifically states the importance of taking account of control surface deflection rates: 'Slow surface actuators will lower the roll performance ... use ... an actual ramp corresponding to the actuator rate limit.' Roll performance is specified in terms of bank angle change in a given time. Using the one degree of freedom roll approximation (16), required deflection rates can be calculated with knowledge of the aircraft's roll damping L_p and its roll control power $L_{\delta,a}$. Aileron deflection rates applied in aircraft design are slightly higher then deflection rates calculated by this method. These higher deflection rates help to satisfy requirements from Automatic Flight Control Systems (AFCS).

MIL-STD-1797 Chapter 4.2.1.2 alternative C presents a method to evaluate short-term pitch response by means of a specified pitch rate response to a step pitch controller deflection. Required elevator deflection rates can be calculated from the effective time delay t_l specified

in MIL-STD-1797 applying the two-degree-of-freedom short-period approximation (16). Calculated deflection rates are in good agreement with pilot observations as indicated e.g. in (17). Nevertheless, AFCS can require deflection rates much higher than those calculated for manual flight with above procedure.

An approach for calculating rudder deflection rates can be based on MIL-STD-1797 Chapter 4.6.5 'Yaw axis response to asymmetric thrust during takeoff run': 'During the takeoff run it shall be possible to maintain a straight path on the takeoff surface without deviations of more than 30 ft from the path originally intended, following sudden asymmetric loss of thrust.' This MIL-requirement is identical to a statement in FAR/JAR 25.149 .

2.3 Flight Control Configuration

Often, already during aircraft preliminary design a decision is made about the type of 'flight control architecture' foreseen for the new aircraft: The flight control architecture might be e.g. a conventional one or a Fly By Wire (FBW) flight control system with a certain number of control surfaces and actuators. In addition, an optimum 'flight control configuration' has to be found. The 'flight control configuration' specifies the allocation of energy systems and command sources to the actuators. This can most easily be explained by looking at an example. **Fig. 4** shows the flight control configuration of primary wing surfaces of the Airbus A320. Each square symbolizes one flight control actuator. Spoilers are operated only by one actuator each. Left and right aileron are operated by two actuators each. A letter shows with which hydraulic system the actuator is connected (G = green, B = blue, Y = yellow). Furthermore, it is indicated which flight control computer commands the respective actuator (ELAC 1, ELAC 2, SEC 1, SEC 2, SEC 3). The question can be raised which flight control configuration (allocation of e.g. hydraulic systems and flight control computers to the actuators) yields optimum performance (= manoeuvrability) under normal operation and failure cases. Dwelling on an idea presented in (18) resulted in an algorithm as follows.

Manoeuvrability about the roll axis of an aircraft is frequently stated by means of the steady state roll rate p_{ss} and can be calculated as a function of available ailerons (i=1 to n) and available spoilers (j=1 to m), roll damping L_p , roll power of respective ailerons $L_{\delta,a,i}$ and spoilers $L_{\delta,s,j}$ and maximum surface deflections of respective ailerons ($\delta_{a,i,max}$) and spoilers ($\delta_{s,i,max}$) for a chosen flight condition

$$p_{ss} = -\frac{1}{L_p} \cdot \left(\sum_{i=1}^{n} L_{\delta_{a_i}} \cdot \delta_{a_{i_{max}}} + \sum_{j=1}^{m} L_{\delta_{s_j}} \cdot \delta_{s_{j_{max}}} \right) \quad . \tag{7}$$

Obviously, a control surface is available and able to operate if at least one actuator operates. An actuator is able to operate if the device itself is working and if it is connected to at least one functioning energy system (e.g. a hydraulic system) and at least one functioning command source (e.g. a flight control computer).

The expected value $E(p_{ss})$ of achieved steady state roll rate p_{ss} for all failure states (including normal operation) ω_i for i = 1 to l is

$$E(p_{ss}) = \sum_{i=1}^{l} p_{ss}(\omega_i) \cdot P(\omega_i) \quad . \tag{8}$$

The number l of possible system states ω_i is

$$l = 2^{(p+q+r)} \quad . \tag{9}$$

For the A320 example presented above considering roll, $p = 3$ (number of energy systems), $q = 5$ (number of command sources), $r = 14$ (number of actuators). p_{ss} - the steady state roll rate for a given failure state ω_i - follows from equation (7), $P(\omega_i)$ is the probability of the respective failure state ω_i . The probability P of an item or system being operative (the reliability) is

$$P = R(t) = e^{-\lambda \cdot t} \tag{10}$$

and the probability P for failure is

$$P = F(t) = 1 - e^{-\lambda \cdot t} \quad . \tag{11}$$

Table 2 presents some failure rates λ for preliminary flight control configuration design. For general considerations, the reliability R and probability of failure F are calculated for a time t of one hour.

Table 2: Failure rates λ for preliminary flight control configuration design.

item/system	failure rate λ per flight hour
hydraulic system	10^{-4}
flight control computer	10^{-4}
actuator with electro-hydraulic servo-valve	10^{-5}
actuator with mechanical hydraulic servo-valve	10^{-6}
mechanical control linkage	10^{-7}

It can be assumed that failures of actuators, energy systems and command sources are independent of each other. Therefore, the probability of a failure state ω_i can be calculated by multiplying the probabilities of the elementary events $P_{e,u}$ (probability of an energy system u being either operative or failed), $P_{c,v}$ (probability of a command source v being either operative or failed) and $P_{a,w}$ (probability of an actuator w being either operative or failed):

$$P(\omega_i) = \prod_{u=1}^{p} P_{e_u} \cdot \prod_{v=1}^{q} P_{c_v} \cdot \prod_{w=1}^{r} P_{a_w} \quad . \tag{12}$$

The expected value of achieved steady state roll rate $E(p_{ss})$ (equation (8)) helps to find an answer to the question raised above:

The optimum flight control configuration (= allocation of energy systems and command source to the actuators) is the one which produces the highest expected value of steady state roll rate.

Note however:

1.) The number l of possible system states ω_i can be quite high. For the A320-example presented above l = 4194304 . Today, even for a fast computer it is quite a task to evaluate all these system states and to calculate the expected value $E(p_{ss})$. For a quick comparison of different flight control configurations in preliminary design, the effort can be considerably reduced when initially neglecting the effect of the actuators in the investigation. This means assuming that actuators themselves are 100% reliable ($R_{a,w}$ = 1; $P_{a,w}$ = 1). Consequently, the number of possible system states reduces to 256 in the above example.

2.) Due to aircraft reliability, expected values $E(p_{ss})$ will always be close to the maximum steady state roll rate $p_{ss,max}$. The term $p_{ss,max}$ - $E(p_{ss})$ helps to easily distinguish the effect of different flight control configurations.

3.) A flight control configuration with optimum $E(p_{ss})$ may not be the first choice. Other design factors like routing of hydraulic tubes and demands placed on hydraulic systems may be in contrast to flight mechanical considerations.

The method presented can also be applied to aircraft pitch and yaw axis and related control surfaces. Prerequisite is the definition of manoeuvrability for these axes. However, pitch and yaw axis have less related control surfaces and actuators and hence an optimum flight control configuration does not necessarily demand a computerized approach.

2.4 Hydraulic system steady state calculation

The complexity of the aircraft hydraulic systems does not allow for a precise direct layout of its components. On the other hand, the effort of applying a simulation taking account of the dynamic behaviour of the whole hydraulic system can not be justified. For that reason, a steady state calculation provides a sound compromise between necessary detail and modelling effort required from the aircraft engineer.

The hydraulic module offers the possibility to perform a steady state analysis of the aircraft hydraulic system during different flight phases under normal and failure cases. The program was especially designed for the aircraft industry and includes - in addition to general hydraulic components - models of aircraft components like power transfer units (PTU) and pressure maintaining valves. The spool valve position of a servo valves is generally not known a priori since it is a function of controller output. For the steady state analysis, the spool valve positions are iteratively calculated as a function of actuator piston speeds (following from control surface deflection rates) and supply pressure. The hydraulic module calculates pressure at all nodes and flow through every component of the system.

This procedure enables an optimum layout of aircraft hydraulic components. Especially pumps and actuators can be dimensioned much more precisely than in the past. Formerly the

pumps were dimensioned by a simple summation of estimated flow demands. Now the flow demands can be accurately calculated as a function of the pressure distribution in the system. Line sizing and routing can be refined. Excessive pressure drops can be spotted. Design oversights can be discovered by checking the general functioning of the system. This helps to eliminate potential testing and redesign expenditures.

The module applies the Linear-Theory-Method using linearized p-q-equations for its core calculation (19). For all nodes j in the system, the continuity equation yields

$$\sum_{i=1}^{k} C_x' (p_i - p_j) + q_j = 0, \qquad \text{for all nodes } j = 1, ..., J \quad . \tag{13}$$

q_j is the external flows at node j, the p_i are the pressures in k different nodes connected with j, the linearized conductance C'_x is calculated from

$$C_x' = \frac{|p_i - p_j|^{\frac{1}{n} - 1}}{R_x^{\frac{1}{n}}} \quad . \tag{14}$$

with $n = 2$ and the resistance of the hydraulic component R_x connencting i and j. The system of linear equations is solved iteratively with changing C'_x for the unknown pressures in the nodes by *Gauss-Elimination* with partial pivoting and scaling. To prevent the iteration from overshooting, a certain amount of damping is applied.

3 PRELIMINARY DESIGN OF FLIGHT CONTROL ACTUATORS

Still most common on today's aircraft are linear hydraulic servo actuators consisting of a cylinder and a servo valve either electrically or mechanically controlled, powered by a central hydraulic system. A preliminary layout of these actuator types will be detailed below. Integrated hydraulic Actuator Package (IAP) systems might play a more important part in future aircraft. Preliminary layout of certain IAP designs is supported in the CAE tool although not further discussed at this point.

3.1 Static actuator layout

Installation space is usually very limited for actuator integration. The CAE tool supports actuator integration and static actuator layout by:

1.) Calculation of available installation space from aircraft design data.
2.) Check of unobstructed actuator travel within available installation space. This includes:
   - a first guess of piston area and effective moment arm from maximum hinge moment requirements and working pressure $p_0 = p_s - p_r$
     (for layout use $p_0 = 195$ bar for a 206 bar hydraulic system),
   - calculation of overall actuator dimensions from statistical or known data,
   - an integration strategy specified by the aircraft engineer.

Piston area, stroke, effective moment arm and moment arm versus deflection angle result from this computer dialogue.

3.2 Selection of servo valve

For flight control actuation systems specific load (F) - rate ($\dot{\delta}$) combinations must be satisfied:

1.) maximum hinge moment at zero rate, (This is sizing the cylinder, see Chapter 3.1 .)
2.) maximum power condition combining a high surface rate with a hinge moment load,
3.) a maximum no-load rate.

Load / rate combination 2.) should size the servo valve. Nevertheless, in practice load / rate combination 3.) often dictates the size of the valve. It can hardly be justified if combination 3.) dimensions the valve and load / rate combinations should be reconsidered. The required size of the servo valve defined by its required nominal rated flow $q_{nom,req}$ is calculated with the dimensioning load / rate combination from

$$q_{nom_{req}} = A \cdot h \cdot \dot{\delta} \cdot \sqrt{\frac{p_{nom}}{p_s - p_r - F/A}} \quad . \tag{15}$$

p_{nom} : nominal pressure loss, A : piston area, h : effective moment arm, $\dot{\delta}$: deflection rate [rad], p_s : supply pressure, p_r : return pressure, F : actuator load.

3.3 Specification of dynamic actuator performance

The *Society of Automotive Engineers* has laid down a frequently quoted standard for actuator specifications with ARP 1281 'General Specification for Hydraulic Power Operated Aircraft Flight Control Actuators' (20). For gain and phase margins ARP 1281 refers to MIL-F-9490 (21). Key dynamic characteristics for preliminary actuator design from these sources are listed in **Table 3**. Limits to the frequency response are specified for military aircraft as boundaries in the *Bode* diagram. For civil aircraft common practise is to specify amplitude ratio and phase shift just for single input frequencies (**Table 4**).

Table 3: Key dynamic characteristics for preliminary actuator design extracted from ARP 1281 and MIL-F-9490D.

Parameter	Requirement
gain margin	6 db (without aerodynamic damping) [1]
phase margin	45° [1]
frequency response	An input of 2 ... 5% amplitude and an input of 10 ...25% amplitude shall be used. The output at these inputs shall be within specified maximum and minimum limits.
transient response	A step input of 5%, 10% and 25% of total amplitude, for both loaded and unloaded conditions shall be used.

[1] If the eigenfrequency of the actuator with engaged AFCS is higher than the first aero-elastic mode, see MIL-F-9490D for further information.

Table 4: Dynamic response characteristics commonly specified for civil aircraft.

Frequency	Amplitude Ratio	Phase Shift
0.5 Hz	-3 db ... 2 db	< 20 °
2.0 Hz	≤ 2 db	< 50 °

3.4 Actuator dynamics

Actuator dynamics are calculated for the control loop presented in **Fig. 5**. $F_2(s)$ is the transfer function which describes the main stage of the servo valve and the cylinder. Derivation of $F_2(s)$ is a summary based on (22) and considers an actuator with attachment stiffness c_{rl} between ram and load and attachment stiffness c_{rs} between ram and structure. The valve characteristic is linearized giving a flow rate

$$q = c_q \cdot y + c_{qp} \cdot p_l \quad . \tag{16}$$

y : valve spool travel, p_l : load pressure $p_l = F/A$. c_{qp} depends on flow gain c_q and pressure gain c_p : $c_{qp} = c_q / c_p$. The load $F = c_a \cdot x$ is assumed to be proportional to piston travel x . V_0 is the total volume of one actuator chamber with the piston in its mid position. V_0 is considered to be constant which is equivalent to assuming small amplitudes of piston travel x . A calibrated laminar flow orifice can be considered between both actuator chambers producing a pressure drop $\Delta p = q / k_l$. Such an orifice can be applied to increase damping.

$F_1(s)$ introduces the time-lag due to the first stage of an electro-hydraulic servo valve by means of a P-T_1-element. In case of a mechanical hydraulic servo valve, $F_1(s) = 1$. k is the controller gain. k is calculated from specifications of actuator dynamics as detailed in Chapter 3.5. For the mechanical hydraulic servo valve, k describes the gain originating from the linkage assembly (**Fig. 6**).

$$F_1(s) = \frac{k_1}{T s + 1} \tag{17}$$

T : time constant of first stage of electro-hydraulic servo-valve; $T = 0$, $k_1 = 1$ for mechanical hydraulic servo-valve.

$$F_2(s) = \frac{k_2 \cdot N(\hat{y}, y_{max})}{\epsilon + s \cdot \left[1 + \mu + \frac{2D}{\omega_n} s + \frac{1}{\omega_n^2} s^2\right]} \tag{18}$$

with the describing function $N(\hat{y}, y_{max})$ from harmonic analysis taking account of limited valve spool travel

$$k_2 = \frac{c_q}{A} \quad , \tag{19}$$

$$\epsilon = \frac{c_a}{A^2}\left(k_l + c_{qp}\right) + k_2 \frac{c_a}{c_{rl}} \quad , \tag{20}$$

$$\mu = \frac{d}{A^2}\left(k_l + c_{qp}\right) + \frac{c_a}{c_h} + \frac{c_a}{c_{rl}} + \frac{c_a}{c_{rs}} \quad . \tag{21}$$

μ consists of values which are small compared to other values in the transfer function. For this reason μ is often neglected. For computer applications, the inclusion of μ does not cause much additional effort. The hydraulic stiffness of the cylinder is

$$c_h = \frac{2\,K\,A^2}{V_0} \tag{22}$$

where K represents the bulk modulus. The characteristic angular frequency ω_n is calculated from

$$\omega_n = \sqrt{\frac{1}{\frac{m}{c_h} + \frac{m}{c_{rl}} + \frac{m}{c_{rs}}}} \tag{23}$$

with m as the moving mass. The damping ratio is

$$D = \frac{\omega_n}{2}\left(\frac{k_l\,m}{A^2} + \frac{c_{qp}\,m}{A^2} + \frac{d}{c_h}\right) \quad . \tag{24}$$

The damping coefficient

$$d = d_p + d_a + d_v \tag{25}$$

can include damping of a parallel actuator in bypass or damping mode d_p , aerodynamic damping d_a and normal viscous damping d_v . Coulomb friction is neglected. When considering damping of a parallel actuator with a turbulent flow orifice, a linearization based on harmonic analysis given in (22) can be applied to find iteratively the damping coefficient from the amplitude of the piston position $\hat{x}$

$$d_p = \frac{\hat{x} \cdot \omega \cdot A^3}{1.113 \cdot k_t^2} \quad . \tag{26}$$

3.5 Calculation of controller gain k

Stability based on a specified gain margin M_m has to be achieved under all circumstances. Therefore, the controller gain k is calculated without aerodynamic damping ($d_a = 0$). Furthermore, small input amplitudes $\hat{x}_c$ are assumed which is equivalent to considering $N(\hat{y}\ ,\ y_{max}) = 1$ and $d_p = 0$. Required are gain margin frequency

$$\omega_M = \sqrt{\frac{\omega_n^2 (T \epsilon + 1 + \mu)}{2 \omega_n T D + 1}} \quad , \tag{27}$$

amplitude ratio of the open loop (excluding the controller gain k itself)

$$M_o(\omega) = \frac{k_1 \cdot k_2}{\sqrt{U^2(\omega) + V^2(\omega)}} \quad , \tag{28}$$

$$U(\omega) = - T \omega^2 (1 + \mu) + T \frac{\omega^4}{\omega_n^2} + \epsilon - \frac{2 D \omega^2}{\omega_n} \quad , \tag{29}$$

$$V(\omega) = \omega \cdot \left(T \epsilon - \frac{T \omega^2 2 D}{\omega_n} + 1 + \mu - \frac{\omega^2}{\omega_n^2} \right) \tag{30}$$

for finally obtaining the controller gain

$$k = \frac{1}{M_o(\omega = \omega_M) \cdot M_m} \quad . \tag{31}$$

3.6 Checking the phase margin

The phase margin frequency ω_Φ has to be found iteratively from

$$k^2 \cdot k_1^2 \cdot k_2^2 - U^2(\omega_\Phi) - V^2(\omega_\Phi) = 0 \quad . \tag{32}$$

The phase is

$$\Phi(\omega) = \arctan\left(- \frac{V(\omega)}{U(\omega)} \right) \tag{33}$$

and the phase margin Φ_m a function of the phase at the phase margin frequency

$$\Phi_m = 180^\circ + \Phi_o(\omega = \omega_\Phi) \quad . \tag{34}$$

3.7 Checking the frequency response

The closed loop *Bode* diagram consist of amplitude ratio

$$M_c(\omega) = \frac{k \cdot k_1 \cdot k_2 \cdot N(\hat{y}, y_{max})}{\sqrt{W^2(\omega) + V^2(\omega)}} \tag{35}$$

and phase

$$\Phi_c(\omega) = \arctan\left(-\frac{V(\omega)}{W(\omega)}\right) \tag{36}$$

with

$$W(\omega) = k \cdot k_1 \cdot k_2 \cdot N(\hat{y}, y_{max}) + U(\omega) \quad , \tag{37}$$

and $\hat{y}(\omega)$ iteratively from

$$\hat{y}(\omega) = k \cdot k_1 \cdot M_e(\omega) \cdot \hat{x}_c \tag{38}$$

and amplitude ratio $\hat{e}/\hat{x}_c = M_e(\omega)$:

$$M_e(\omega) = \frac{\sqrt{[U(\omega) \cdot W(\omega) + V^2(\omega)]^2 + [V(\omega) \cdot W(\omega) - U(\omega) \cdot V(\omega)]^2}}{W^2(\omega) + V^2(\omega)} \tag{39}$$

and with describing function $N(\hat{y}, y_{max})$ e.g. from (23) :

$$N(\hat{y}, y_{max}) = \frac{2}{\pi}\left[\arcsin\left(\frac{y_{max}}{\hat{y}}\right) + \frac{y_{max}}{\hat{y}}\sqrt{1 - \left(\frac{y_{max}}{\hat{y}}\right)^2}\right] \quad . \tag{40}$$

3.8 Example calculation

The inboard aileron of the *Airbus A340* is used to illustrate equations in Chapter 3.5 to 3.7 . Calculations are performed with *Airbus* geometric and servo valve data, no load and reasonable assumptions on structural stiffness, and viscous damping. A gain margin of at least 6 db is achieved for all flight phases with a controller gain $k = 0.95$ A/m. The gain margin is calculated assuming small amplitudes and neither considering aerodynamic damping ($d_a = 0$; i.e. aircraft on ground) nor damping of the parallel actuator ($d_p = 0$). With above controller gain, the phase margin $\Phi_m = 87°$ which is within specified limits (Table 3). **Fig. 7** shows the closed loop *Bode* diagram with

1.) gain response for
   a) small amplitudes $\hat{x}_c < x_{max}$ (i.e. $N(\hat{y}, y_{max}) = 1$; $d_p = 0$),
   b) maximum amplitude $\hat{x}_c = x_{max}$ and associated valve spool limitations and turbulent flow damping by the parallel actuator;

2.) phase response.

The resulting *Bode* diagram satisfies the conditions of Table 4.

4 IMPLEMENTATION

The CAE-tool under development is conventionally programmed, though attempts have been made to apply Artificial Intelligence (expert systems, configuration systems) to solve problems similar in nature to the ones presented here (24), (25). The CAE-tool can be classified as Decision Support System. The tool allows the systems engineer to work closely

with the computer when it comes to

- o retrieving information,
- o calculating system characteristics,
- o designing alternative solutions,
- o selecting a suitable solution among considered alternatives.

An up to date programming concept ensures the development of a user friendly and comfortable product: Hardware independent programming is based on ANSI C. A User Interface Management System (UIMS) facilitates the programming of an interactive Graphical User Interface (GUI). An incorporated hypertext system provides the user with technical information to his problems in a context sensitive way. An incorporated plot program helps to visualize the results. The independent program modules (Fig. 1) exchange information via a common, universal data base.

5 CONCLUSION

Aircraft utility systems fly successfully on modern aircraft. Nevertheless, it seems that standard design methodologies are often not available. This paper tries to contribute to the process of establishing these methodologies. Modern software technology should be applied to make this knowledge easily accessible for systems engineers.

REFERENCES

(1) MOIR, I.; SEABRIDGE, A.: Aircraft Systems, 1992, (Longman, Essex).

(2) AIR TRANSPORT ASSOCIATION OF AMERICA (ed.): Specification for Manufacturers' Technical Data, ATA Specification 100, Washington D.C., 1981.

(3) ROSKAM, J.: Airplane Design, Part 1-8, Ottawa, Kansas, 1990.

(4) DARCorp: Advanced Aircraft Analysis, Design , Analysis and Research Corporation, 120 East Ninth Street, Suite 2, Lawrence, Kansas, 66044, USA. - Product Information.

(5) RAYMER, D. P.: Aircraft Design: A Conceptual Approach, AIAA Education Series, Washington DC, 1989.

(6) RAYMER, D. P.: RDS - A PC-based Aircraft Design, Sizing, and Performance System. AIAA Aircraft Design Systems Meeting, Hilton Head, South Carolina, 1992 (AIAA, Washington).

(7) SCHOLZ, D.: Betriebskostenschätzung von Flugzeugsystemen als Beitrag zur Entwurfsoptimierung, DGLR-Jahrestagung, Bonn, 1995 (DGLR, Bonn).

(8) HOAK, D. E.; et al: USAF Stability and Control DATCOM, Flight Control Division, Air Force Flight Dynamics Laboratory, WPAFB, Ohio, 1969.

(9) ESDU INTERNATIONAL (ed.): Controls and Flaps, Engineering Sciences Data, Aerodynamic Sub-Series, Vol. 5b, 1989, (ESDU, London).

(10) JOINT AVIATION AUTHORITIES COMMITEE: Joint Aviation Requirements, Part 25, Large Aeroplanes, 1989. - Printed by: Civil Aviation Authority, Cheltenham, UK.

(11) ROSKAM, J.: Airplane Design, Part 6, Ottawa, Kansas, 1990.

(12) WILMERS, W.: Entwicklung eines Programms zur Berechnung von Scharniermomenten an Steuerflächen von Flugzeugen, Technical University Hamburg-Harburg, Aircraft Systems Engineering, Project, 1994.

(13) RAYMOND, E. T.; CHENOWETH, C. C.: Aircraft Flight Control Actuation System Design, 1993, (Society of Automotive Engineers, Warrendale, USA).

(14) MIL-F-8785C, Military Specification, Flying Qualities of Piloted Airplanes, 1980. - Available from: London Information, Index House, Ascot, Berkshire SL5 7EU, UK.

(15) MIL-STD-1797, Flying Qualities of Piloted Vehicles, Draft, Wright-Patterson AFB, Ohio, USA, 1986.

(16) McRUER, D.; ASHKENAS, I.; GRAHMAM, D.: Aircraft Dynamics and Automatic Control, 1973 (Princeton University Press, Princeton, New Jersey).

(17) BUCHHOLZ, J. J.: Time Delay Induced by Control Surface Rate Saturation. Zeitschrift für Flugwissenschaften und Weltraumforschung, 1993, 17, 287 - 293.

(18) TRAVERSE, P.: Dependability of Digital Computers On Board Airplanes. In: AVIZIENIS, A.; LAPRIE, J.C. (ed.): Dependable Computing for Critical Applications, 1991, Vol. 4 (Springer, Wien).

(19) SCHOLZ, D.: Computer Aided Engineering zur Auslegung von Flugsteuerungs- und Hydrauliksystemen, 10. Fachtagung Hydraulik und Pneumatik, Dresden, 1995. (Technische Universität Dresden).

(20) Aerospace Recommended Practice, ARP 1281, Actuators: Aircraft Flight Controls, Power Operated, Hydraulic, General Specification for, 1993, (Society of Automotive Engineers, Warrendale, USA).

(21) MIL-F-9490D (USAF), Military Specification, Flight Control Systems - Design, Installation and Test of Piloted Aircraft, General Specification for, 1975. - Available from: London Information, Index House, Ascot, Berkshire SL5 7EU, UK.

(22) GUILLON, M.: Hydraulic Servo Systems, 1961, (Butterworth, London).

(23) UNBEHAUEN, H.: Regelungstechnik II, 1993, (Vieweg).

(24) ALSINA, J.; FIELDING, J.P.; MORIS, A.J.: Progress Towards an Aircraft Design Expert System. In: MURTHY, T.K.S.; FIELDING, J.P. (Editors): Computer Applications in Aircraft Design and Operation, 1987, (Computational Mechanics Publications, Springer), 229-247.

(25) KOPISCH, M.: XKL - Ein Expertensystem zur Konfiguration des Layouts der Passagierkabine des AIRBUS A340, 2. Deutsche Tagung Expertensysteme, Hamburg, 1993. (Universität Hamburg).

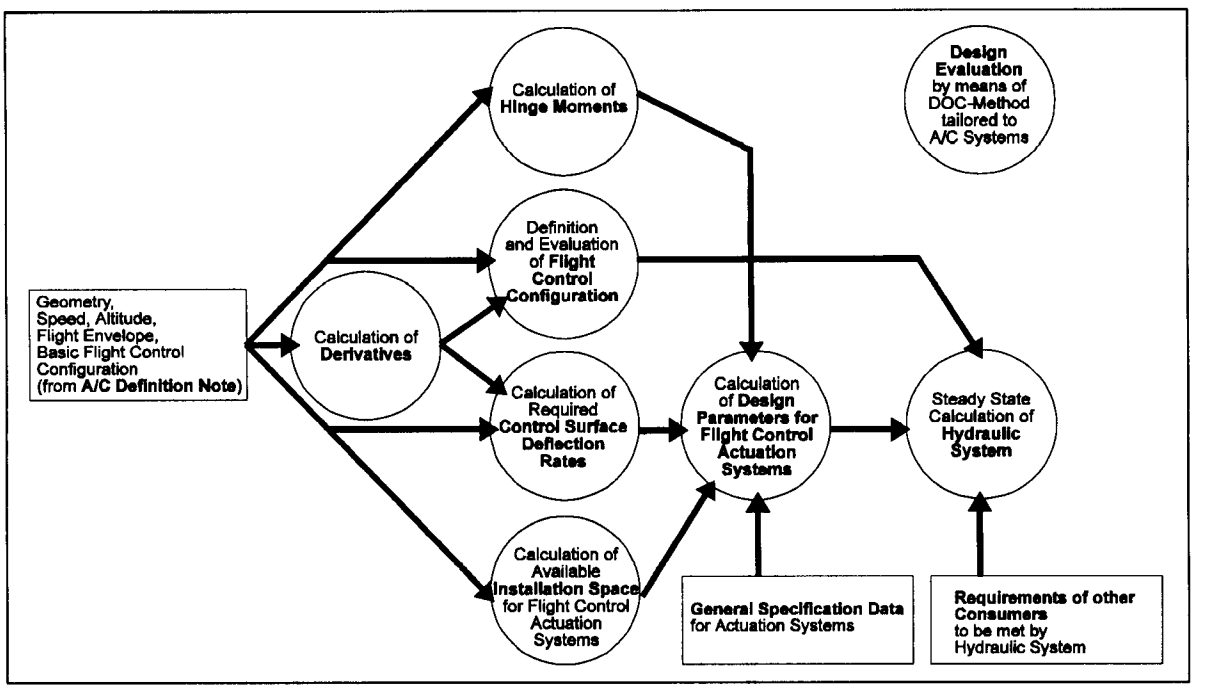

Fig 1 Modules of the Computer Aided Engineering (CAE) Tool for the design of aircraft utility systems

FOR altitude = sea level **TO** maximum service ceiling

FOR v = v_s **TO** (v_{MO} or M_{MO} whichever is lower)

FOR c.g. = c.g. most forward **TO** c.g. most aft

Calculate the deflection angle of the horizontal tail i_{h1} for trimed flight. Allow for a three second runaway in both directions of the horizontal tail or until the stops of the trim system are reached. This yields i_{h2}, i_{h3} .

Calculate for i_{h2} and i_{h3} the required deflection angle δ and the angle of attack α for manoeuvres producing a load factor of n_z = -1 and n_z = **2.5** .

v = (v_D or M_D whichever is lower)

FOR c.g. = c.g. most forward **TO** c.g. most aft

Calculate the deflection angle of the horizontal tail i_{h1} for trimed flight. Allow for a three second runaway in both directions of the horizontal tail or until the stops of the trim system are reached. This yields i_{h2}, i_{h3} .

Calculate for i_{h2} and i_{h3} the required deflection angle δ and the angle of attack α for manoeuvres producing a load factor of n_z = **1.5** .

i_h	horizontal tail incidence angle [deg]	v_D	true air speed, dive [m/s]
M_{MO}	aircraft mach number, maximum operation [-]	v_{MO}	true air speed, maximum operation [m/s]
M_D	aircraft mach number, dive [-]	v_s	true air speed, stall [m/s]
v	true air speed [m/s]	α	angle of attack of horizontal tail [deg]
		δ	deflection angle of elevator [deg]

Fig 2 Calculating a set of horizontal tail angles of attack α and elevator angles δ in search for maximum elevator hinge moments.

altitude = sea level

FOR $n_z = 0$ and $n_z = 2/3 \cdot n_{z,max}$ ($n_{z,max}$ = maximum design load factor)

Calculate α for v = v_A and
$\delta_1 = \delta_{min}$ (maximum deflection down) and
$\delta_2 = \delta_{max}$ (maximum deflection up).

Calculate α for v = v_C and $\delta_1 = \delta_{min} \cdot v_A / v_C$ and $\delta_2 = \delta_{max} \cdot v_A / v_C$.

Calculate α for v = v_D and $\delta_1 = \delta_{min} \cdot 1/3 \cdot v_A / v_D$ and $\delta_2 = \delta_{max} \cdot 1/3 \cdot v_A / v_D$.

v	true air speed [m/s]	α	angle of attack of wing [deg]
v_A	true air speed, manoeuvre speed [m/s]	δ	deflection angle of aileron [deg]
v_C	true air speed, cruise [m/s]		
v_D	true air speed, dive [m/s]		

Fig 3 Calculating a set of wing angles of attack α and aileron angles δ in search for maximum aileron hinge moments.

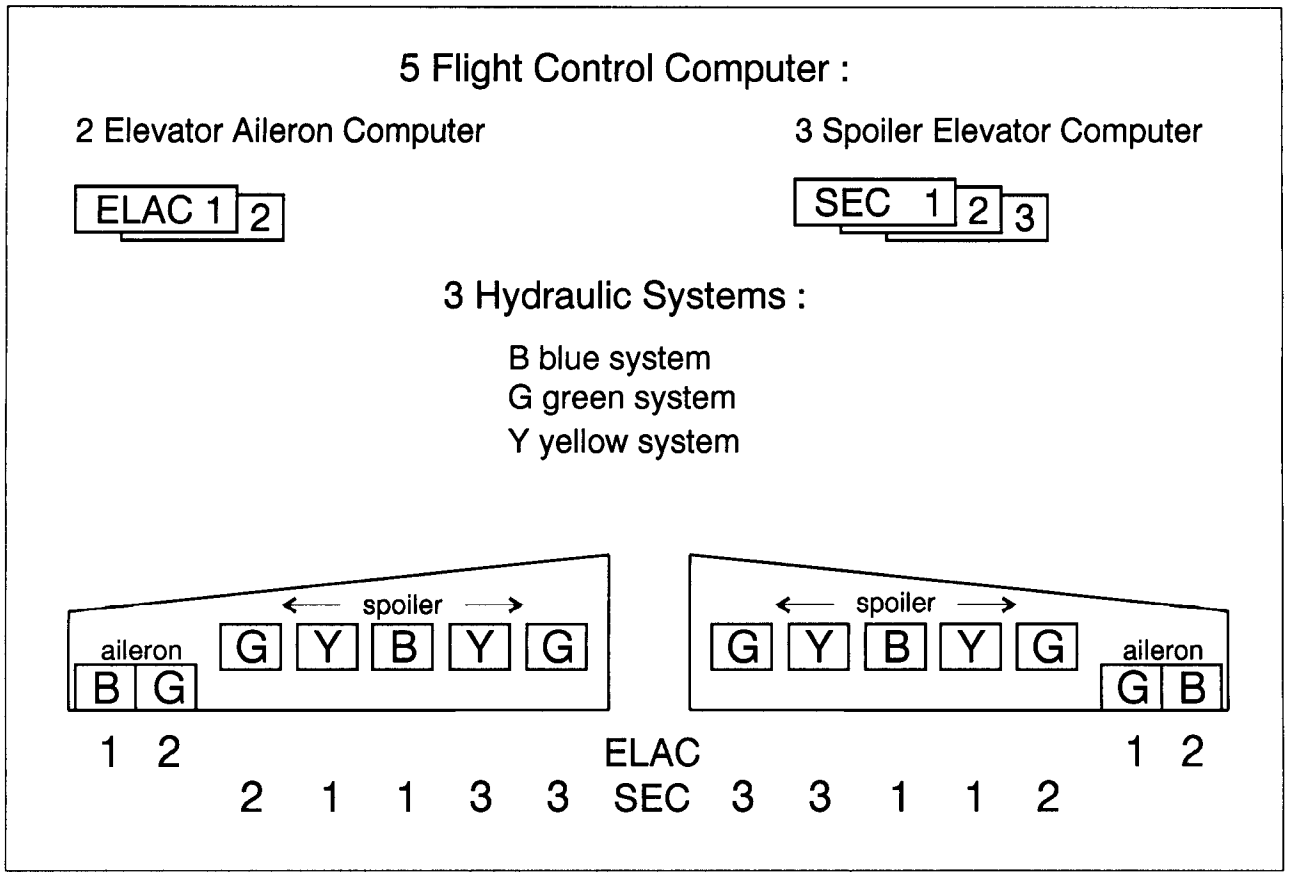

Fig 4 Flight control configuration of primary wing surfaces of the Airbus A320

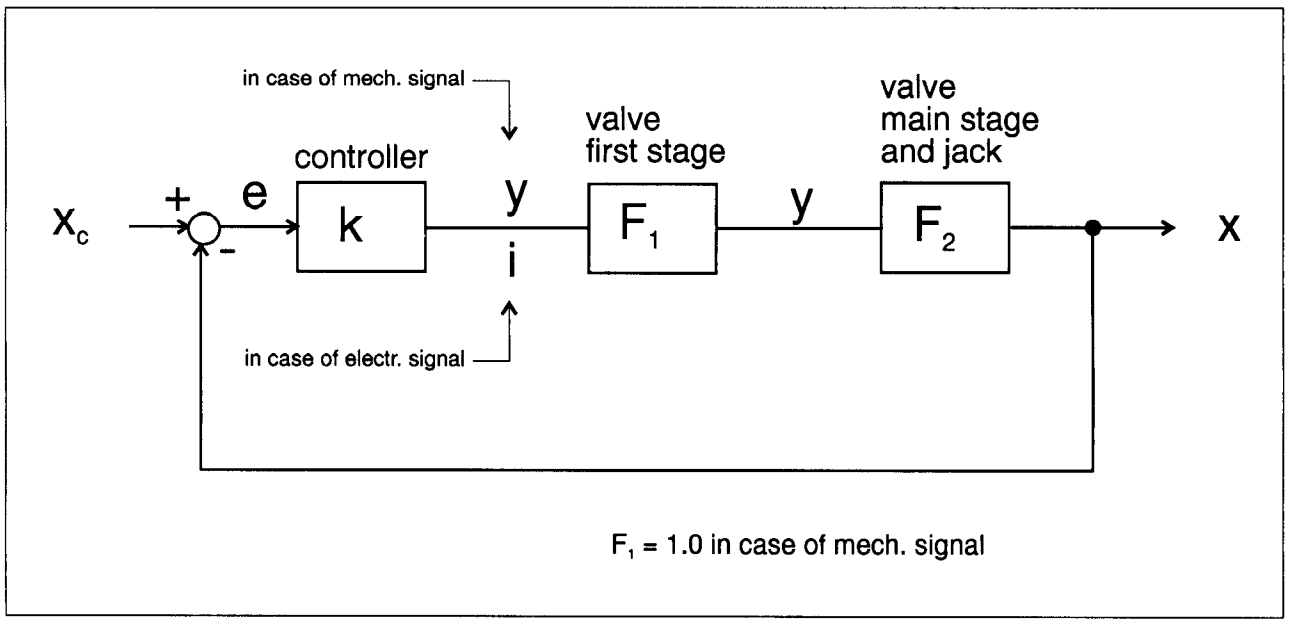

Fig 5 Actuator control loop

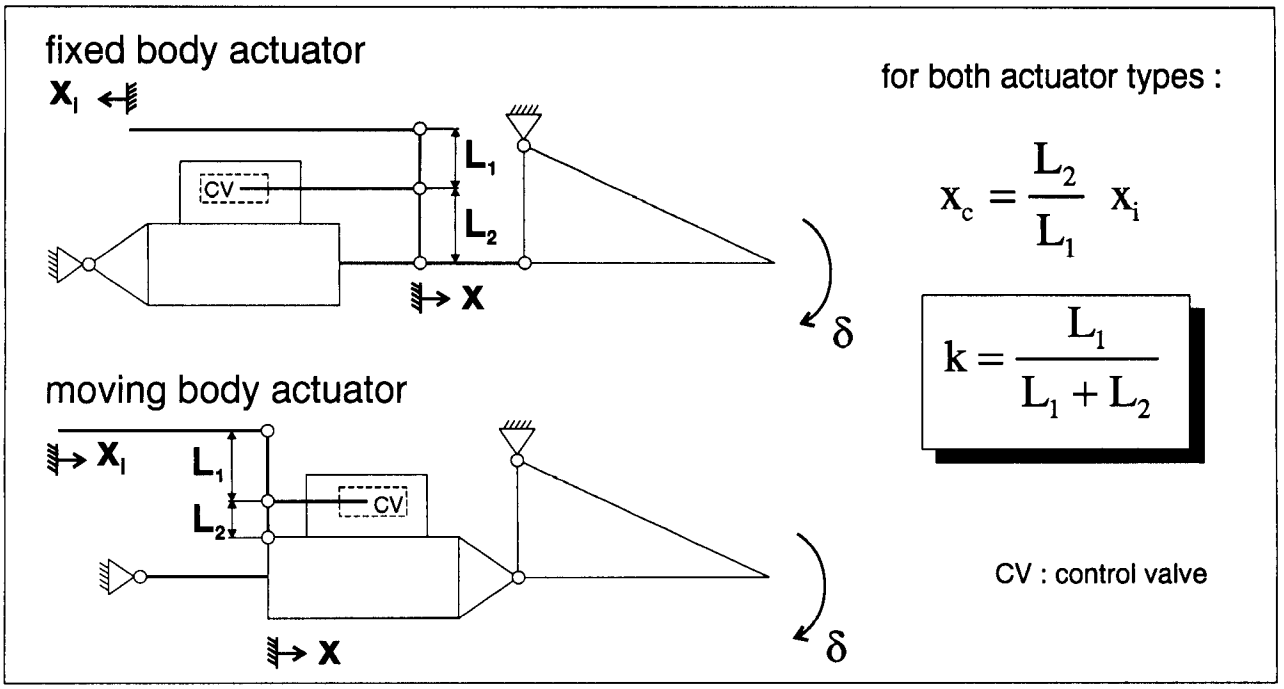

Fig 6 Gain *k* originating from hydraulic servoactuator linkage assembly

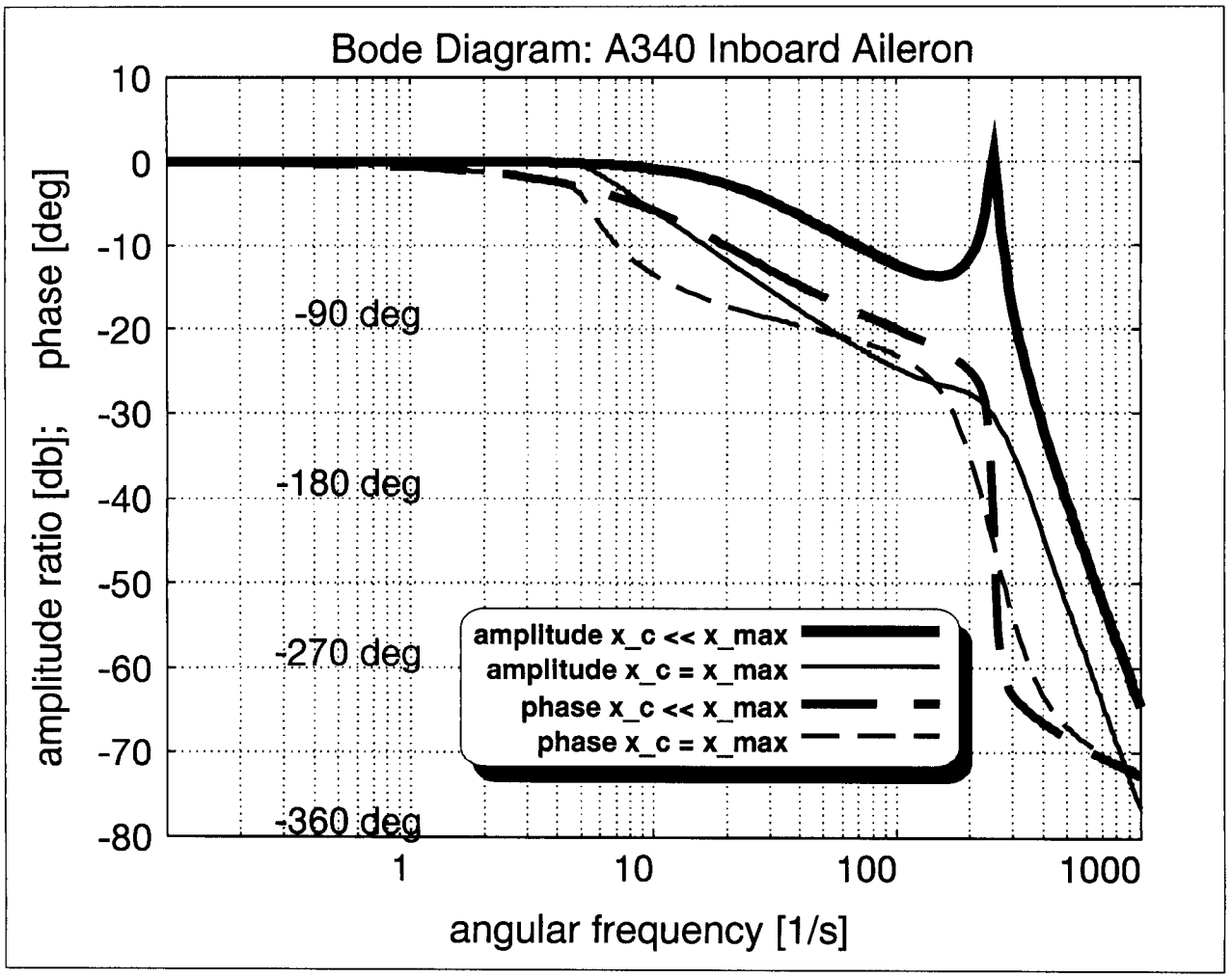

Fig 7 Calculated closed loop Bode diagram of Airbus A340 inboard aileron